MCB
Journals.ASM.org

Sam68 Regulates S6K1 Alternative Splicing during Adipogenesis

Jingwen Song, Stéphane Richard

Terry Fox Molecular Oncology Group and Segal Cancer Center, Bloomfield Center for Research on Aging, Lady Davis Institute for Medical Research, and Departments of Oncology and Medicine, McGill University, Montréal, Québec, Canada

The requirement for alternative splicing during adipogenesis is poorly understood. The Sam68 RNA binding protein is a known regulator of alternative splicing, and mice deficient for Sam68 exhibit adipogenesis defects due to defective mTOR signaling. Sam68 null preadipocytes were monitored for alternative splicing imbalances in components of the mTOR signaling pathway. Herein, we report that Sam68 regulates isoform expression of the ribosomal S6 kinase gene (*Rps6kb1*). Sam68-deficient adipocytes express *Rps6kb1-002* and its encoded p31S6K1 protein, in contrast to wild-type adipocytes that do not express this isoform. Sam68 binds an RNA sequence encoded by *Rps6kb1* intron 6 and prevents serine/arginine-rich splicing factor 1 (SRSF1)-mediated alternative splicing of *Rps6kb1-002*, as assessed by cross-linking and immunoprecipitation (CLIP) and minigene assays. Depletion of p31S6K1 with small interfering RNAs (siRNAs) partially restored adipogenesis of Sam68-deficient preadipocytes. The ectopic expression of p31S6K1 in wild-type 3T3-L1 cells resulted in adipogenesis differentiation defects, showing that p31S6K1 is an inhibitor of adipogenesis. Our findings indicate that Sam68 is required to prevent the expression of p31S6K1 in adipocytes for adipogenesis to occur.

Src-associated substrate during mitosis of 68 kDa (Sam68) is an RNA binding protein that belongs to the conserved STAR (signal transduction activator of RNA) family (1, 2). Sam68 is a sequence-specific RNA binding protein that binds repeats of U(U/A)AA sequences in single-stranded RNA (3, 4). The binding of Sam68 near alternative splice junctions in pre-mRNAs has been shown to regulate splice site selection and regulate the usage of alternative exons (1). Sam68 promotes the inclusion of CD44 variable exon 5 (v5), and interaction of Sam68 with SND1 (staphylococcal nuclease domain 1) enhances v5 inclusion (5, 6). The alternative splicing of Bcl-x is regulated by Sam68 and its interaction with hnRNPA1 and FBI-1, affecting prosurvival and apoptotic pathways (7, 8). Sam68 regulates the epithelial-to-mesenchymal transition by decreasing the presence of an alternative serine/arginine-rich splicing factor 1 gene (*Srsf1*) transcript degraded by nonsense-mediated mRNA decay (9). Sam68 has been shown to regulate alternative splicing of mRNAs during neurogenesis (10) and in cerebellar neurons (11). Stimulation of cerebellar neurons using the glutamate receptor agonist kainic acid was dramatically attenuated without Sam68, indicating that Sam68 is required for activity-dependent alternative splicing of Nrxn1 *in vivo* (11).

The role of Sam68 in alternative splicing has implications for spinal muscular atrophy (SMA) and fragile X-associated tremor/ataxia syndrome (FXTAS). Sam68 promotes the skipping of exon 7, leading to a nonfunctional SMN2 protein, and it was shown that the inhibition of Sam68 enhanced exon 7 inclusion in endogenous *SMN2* and increased survival motor neuron (SMN) levels in SMA patient cells (12). Expanded CGG repeats in the 5′ untranslated region (UTR) of the *FMR1* gene causes FXTAS, and Sam68 association with these repeats in RNA aggregates blocks it from fulfilling its splicing functions (13). The inhibition of Sam68 phosphorylation prevents Sam68 from aggregating with RNA, suggesting that it may be a therapeutic option for FXTAS patients (13).

Sam68 null mice have revealed numerous unexpected physiological roles for Sam68. Male Sam68$^{-/-}$ mice are infertile, with defects in spermatogenesis, a process where Sam68 has been shown to regulate alternative splicing (14) and the polysomal recruitment of specific mRNAs in germ line cells (15). Ablation of Sam68 leads to increased energy expenditure, decreased numbers of early adipocyte progenitors, and defective adipogenic differentiation, resulting in mice having a lean phenotype protected against dietary-induced obesity (16). The lack of Sam68 results in mTOR (mammalian target of rapamycin) intron 5 retention and the production of a short transcript (named mTOR$_{i5}$), leading to reduced mTOR protein levels, which results in defects in insulin-stimulated S6 and Akt phosphorylation (16).

mTOR signaling plays a major role in the regulation of mRNA translation, cell growth, metabolism, and autophagy (17–19). The tuberous sclerosis complex (TSC; tuberous sclerosis 1 and 2 heterodimer) acts as a GTPase-activating protein (GAP) on the Ras-like protein Rheb, which activates the mTOR complex 1 (mTORC1) (20–22), and PRAS40 (proline-rich Akt substrate of 40 kDa) is an inhibitory mediator of mTORC1 signaling. The phosphorylation and inhibition of the TSC and PRAS40 by the upstream kinase Akt (serine/threonine protein kinase B) activate mTORC1 signaling (23–25). Activated mTOR signaling results in phosphorylation of 4EBP1 (initiation factor 4E-binding protein 1) and S6K1 (S6 kinase 1) (18, 19, 26). Active S6K1 phosphorylates the 40S ribosomal protein S6, thereby facilitating mRNA translation, while phosphorylated 4EBP1 promotes the release of eIF4E (eukaryotic translation initiation factor 4E) and initiates translation (26).

In the present manuscript, we identify Sam68 as an RNA bind-

Received 12 December 2014 **Returned for modification** 2 January 2015
Accepted 11 March 2015

Accepted manuscript posted online 16 March 2015

Citation Song J, Richard S. 2015. Sam68 regulates S6K1 alternative splicing during adipogenesis. Mol Cell Biol 35:1926–1939. doi:10.1128/MCB.01488-14.

Address correspondence to Stéphane Richard, stephane.richard@mcgill.ca.

Supplemental material for this article may be found at http://dx.doi.org/10.1128/MCB.01488-14.

doi:10.1128/MCB.01488-14

ing protein that prevents the production of the alternative short isoform of *Rps6kb1*, encoding p31S6K1, in mouse preadipocytes and white adipose tissue (WAT). The binding of Sam68 to an *Rps6kb1* intronic RNA sequence counteracted the alternative splicing effects of the SR protein, SRSF1. Expression of p31S6K1 in preadipocytes inhibited differentiation, while the depletion of p31S6K1 in Sam68-deficient preadipocytes partially restored the adipogenic differentiation defects in a p70S6K1-independent manner. Our findings show that Sam68 is a regulator of *Rps6kb1* alternative splicing during adipogenesis.

MATERIALS AND METHODS

Alternative splicing assessment and real-time PCR. Total RNA was isolated using TRIzol reagent according to the manufacturer's instructions (Invitrogen). Four micrograms of RNA was incubated at 65°C for 5 min and then at 42°C for 1 h with 100 pmol of oligo(dT) primer and 100 U of Moloney murine leukemia virus (M-MLV) reverse transcriptase (catalog no. M1701; Promega) according to the manufacturer's protocol. cDNAs were then amplified by PCR. Endogenous *Rps6kb1* and *Rps6kb1-002* were amplified with the common forward primer 5′-GCA ATG ATA GTG AGG AAT GCT AAG-3′ located in exon 5. The reverse primer for *Rps6kb1* was 5′-GCT GTG TCT TCC ATG AAT ATT CC-3′ located in exon 6, and for *Rps6kb1-002* the reverse primer was 5′-GAA TAG GAG GGC AGA TCC CAT CC-3′ located in exon 6b. For *TSC1* and *TSC1-003* amplification, the common forward primer 5′-GTG GAA GAC ATT AGA AAC TCA TG-3′ was used. The reverse primer sequence for *TSC1* was 5′-AGG TGG ACT GAA CAA CAT CAG C-3′, and for *TSC1-003* it was 5′-TCA ACT ACA AGT AGT ATG TTA TG-3′. The common forward primer for *TSC1* and *TSC1-006* amplification was 5′-GTG GAA GAC ATT AGA AAC TCA TG-3′. The reverse primer sequence for *TSC1* was 5′-AGG TGG ACT GAA CAA CAT CAG C-3′, and for *TSC1-006* it was 5′-ACC CAG CGG TCC ACA CTG ATT TG-3′. For *Rheb* and *Rheb-002* amplification the common forward primer 5′-GAA AGT CCT CAT TGA CAA TTC AG-3′ was used. The reverse primer sequence for *Rheb* was 5′-CTG CCC CGC TGT GTC TAC AAG C-3′, and for *Rheb-002* it was 5′-GTG AGT GTC AGC CCT CAC TCT AC-3′. Endogenous *Rheb* and *Rheb-003* were amplified with the common forward primer 5′-GAT CAG CTA TGA AGA AGG AAA GGC-3′. The reverse primer sequence for *Rheb* was 5′-TTG GAC AGA GTC AGA CGT TAA C-3′, and for *Rheb-003* it was 5′-CAT CAC CGA GCA CGA AGA CTT TC-3′. For *Akt1* and *Akt1-003* amplification, the forward primer sequence for *Akt1* was 5′-GGA GGG CTG GCT GCA CAA ACG AG-3′, and that for *Akt1-003* was 5′-GCC GCT GCG TGA CCT TGG GTG G-3′. The common reverse sequence for both *Akt1* and *Akt1-003* was 5′-CCG CTC TGT CTT CAT CAG CTG GC-3′. For *Rps6kb1* and *Rps6kb1-005* amplification, the common forward sequence used was 5′-TCT CAG AAA CTA GTG TGA ACA G-3′. The reverse primer sequence for *Rps6kb1* was 5′-CAC TGA GAT ACT CGA GGA TGA GG-3′, and for *Rps6kb1-005* it was 5′-ATT AAG ATA TAG CAT AGA GTG AG-3′. For *Deptor* and *Deptor-002* amplification, the common forward primer 5′-ATT GTT GGT GAC GCA GTT GGC TG-3′ was used. The reverse primer sequence for *Deptor* was 5′-AGA TAT GTA ACC TGG TTC TTC CAC-3′, and for *Deptor-002* it was 5′-ACC CAC CTT CCC TCC CAT TAG GTC-3′.

For real-time reverse transcription-PCR (RT-PCR), mouse *Rps6kb1* was amplified with 5′-CGT GGA GTC TGC GGC G-3′ (located in exon 1) and 5′-CAT ATG GTC CAA CTC CCC CA-3′ (located in exon 2), mouse *Rps6kb1-002* was amplified with 5′-TAT GCC TTT CAG ACC GGA GG-3′ (located in exon 5) and 5′-ACC TCC CTA AGA CTG CAC CT-3′ (located in exon 6b), 18S rRNA was amplified with 5′-GTA ACC CGT TGA ACC CCA TT-3′ and 5′-CCA TCC AAT CGG TAG TAG CG-3′, C/EBPα was amplified with 5′-CGC AAG AGC CGA GAT AAA GC-3′ and 5′-GCG GTC ATT GTC ACT GGT CA-3′, GLUT4 was amplified with 5′-TCG TGG CCA TAT TTG GCT TTG TGG-3′ and 5′-TAA GGA CCC ATA GCA TCC GCA ACA-3′, peroxisome proliferator-activated receptor γ (PPARγ) was amplified with 5′-GAA CGT GAA GCC CAT CGA GGA C-3′ and 5′-CTG GAG CAC CTT GGC GAA CA-3′, as previously described (27), and glyceraldehyde-3-phosphate dehydrogenase (GAPDH) was amplified with 5′-AGC CAC ATC GCT CAG ACA C-3′ and 5′-GCC CAA TAC GAC CAA ATC C-3′. Sam68 was amplified with 5′-GTG GAG ACC CCA AAT ATG CCC A-3′ and 5′-AAA CTG CTC CTG ACA GAT ATC A-3′. Moreover, primers for mouse GAPDH, Sam68, C/EBPα, and PPARγ were purchased from Qiagen (Valencia, CA). Real-time quantitative RT-PCR (RT-qPCR) was performed on a 7500 Fast real-time PCR system (Applied Biosystems, Foster City, CA) using SYBR green PCR Mastermix (Qiagen, Valencia, CA). The primer efficiency test using dilutions confirmed that the efficiencies were close to 1.0 for PPARγ, C/EBPα, GLUT4, GAPDH, and 18S rRNA.

Plasmid constructions. The GFP-Sam68 expression vector encoding an N-terminal green fluorescent protein (GFP) was described previously (28). The GFP-SRSF1 expression vector was obtained from Addgene (catalog no. 17990; Cambridge, MA). Gene *Rps6kb1* exon 6, intron 6, and exon 7 were amplified from mouse genomic DNA by PCR using the forward primer 5′-GGG GGA TCC GGA GGA GAA CTA TTT ATG CAG TTA-3′, containing a BamHI site, and the reverse primer 5′-GGG CTC GAG CTT GGT GAT TAA GCA TGA TGT TCT-3′, containing an XhoI site. The DNA fragment was then subcloned in the corresponding site of pcDNA3.1 containing a FLAG epitope tag. The mutation of the Sam68 binding site (SBS) in intron 6 of the minigene was performed in a two-step PCR using primers 5′-ATG ATT CAT GTA ATT CCA AGC AAA ACC ACC TT-3′ (forward primer) and 5′-AAG GTG GTT TTG CTT GGA ATT ACA TGA ATC AT-3′ (reverse primer). The plasmids encoding full-length p31S6K1 were purchased from IDT and subcloned in pcDNA3.1. An expression vector encoding p31S6K1 was kindly provided by Rotem Karni (Hebrew University-Hadassah Medical School). The common forward primer for RT-PCR and RT-qPCR detection of the *Rps6kb1* minigene transcripts was F1 (5′-GAT TAC AAG GAT GAC GAC GAT AAG-3′). The reverse primers for RT-PCR detection were as follows: R1, 5′-AGG ATG GAG GGT GTG TCC TAG AGG-3′; R2, 5′-CTT GGT GAT TAA GCA TGA TGT TCT-3′. The reverse primers for RT-qPCR detection were the following: R3, 5′-CAA TTC AAG GAA ATT CTG CAG TG-3′; R4, 5′-GCC ATG GAG ATT TCA GCC AAG-3′.

Synthetic RNA oligonucleotides. The RNA oligonucleotides with 3′ biotin tags were synthesized and purchased from IDT. The sequences of these oligonucleotides are as follows: Rps6kb1-SBS, 5′-CAU GAU UCA UGU AAU UAA AAG CAA AAC CAC CUU C-3′-biotin; Rps6kb1-SBSmut, 5′-CAU GAU UCA UGU AAU UCC AAG CAA AAC CAC CUU C-3′-biotin.

Preadipocyte differentiation and WAT. Sam68-deficient 3T3-L1 cells were generated using pRetrosuper harboring a short hairpin RNA (shRNA) targeting Sam68 (Sam68sh), and pRetrosuper 3T3-L1 cells were used as a control, as described previously (16). Preadipocyte 3T3-L1 adipogenic differentiation was performed as described previously (29). The cells were fixed with 3% formaldehyde and 0.025% glutaraldehyde and incubated with Oil Red O solution (Sigma-Aldrich, St. Louis, MO). Cell extracts were prepared and analyzed as described previously (16). Antibodies for Sam68 (Millipore), p70 S6K (BD Transduction Laboratories, Cell Signaling), GFP (Roche), SRSF1 (Santa Cruz), FLAG M2, β-actin, and β-tubulin (Sigma) were purchased.

Stable 3T3-L1 clones overexpressing p31S6K1 were generated as follows. Cells were transfected with either pcDNA3.1 or pcDNA3.1 FLAG-p31 plasmid constructs. At 48 h posttransfection, G418 was added to the medium, and individual clones were selected several weeks later. The expression level of p31S6K1/FLAG was assessed by immunoblotting.

RNA interference and transfection. The following siGENOME SMARTpool small interfering RNAs (siRNAs) were ordered from Dharmacon/Thermo Scientific: human KHDRBS1 (Sam68) (catalog no. M-020019-00-0010), mouse KHDRBS1 (Sam68) (catalog no. M-065115-01-0010), human SRSF1 (catalog no. M-018672-00-0005), and mouse SRSF1 (catalog no. M-040886-01-0005). Mouse RPS6KB1 (p70/p31) siGENOME set of four siRNAs (catalog no. MQ-040893-02-0002) was

ordered from Dharmacon/Thermo Scientific. The following siRNAs were also ordered from Dharmacon/Thermo Scientific: mouse p31 siRNA-A sense sequence (5′-GCU CUU CAC UGC AGA AUU UUU-3′) and antisense sequence (5′-AAA UUC UGC AGU GAA GAG CUU-3′), mouse p31 siRNA-B sense sequence (5′-ACA CAG AAG CUG CAU UUA AUU-3′) and antisense sequence (5′-UUA AAU GCA GCU UCU GUG UUU-3′), and siRNA targeting GFP (siGFP) sense sequence (5′-AAC ACU UGU CAC UAC UUU CUC UU-3′) and antisense sequence (5′-GAG AAA GUA GUG ACA AGU GUU UU-3′).

For siRNA transfections, typically cells were plated in six-well plates and transfected with 100 nM siRNA using Lipofectamine RNAiMAX (siRNA), as recommended by the manufacturer (Invitrogen). HEK293 cells plated in six-well plates were transfected using Lipofectamine 2000. Each well received a total of 5 μg with GFP-SRSF1 (0, 0.25, 1, and 2 μg), GFP-Sam68 (1 μg), and 2 μg of the indicated minigene; an empty vector was used to compensate the amount of transfected DNA in Fig. 7C and D.

RNA binding assays. 3T3-L1 cells were lysed in 1 ml of cell lysis buffer (20 mM Tris-HCl, pH 8.0, 150 mM NaCl, 1% Triton X-100, 40 units/ml RNaseOUT, supplemented with Roche Complete Mini, EDTA-free protease inhibitor) and incubated for 15 min at 4°C. Lysates were cleared by centrifugation, and 5 μl of 100 μM biotinylated RNA was added to the lysates and incubated at 4°C for 60 min with constant end-over-end mixing with streptavidin-Sepharose beads. The beads were washed three times with lysis buffer and once with 1× phosphate-buffered saline (PBS). Protein samples were analyzed on SDS-polyacrylamide gels and transferred to nitrocellulose membranes for immunoblotting.

Immunoprecipitation. Transfected HEK293 cells were lysed in buffer containing 1% Triton X-100, 150 mM NaCl, 20 mM Tris (pH 7.5), and proteinase inhibitor (Roche) for 15 min on ice. Total cell lysates were clarified by centrifugation for 10 min at 10,000 × *g* at 4°C. The lysates were incubated with the indicated antibodies (see Fig. 4D) for 1 h or overnight at 4°C, and then 20 μl of 50% protein A/G slurry was added. The mixture was incubated for 30 min at 4°C. The protein A/G-Sepharose beads were washed three times with lysis buffer and once with 1× PBS. The samples were boiled and subjected to standard Western blot analysis.

UV CLIP. 3T3-L1 cells (pRetrosuper and Sam68sh cells) were treated with 4-thiouridine to a final concentration of 100 μM added directly to the cell culture medium 8 h prior to cross-linking. The cells were washed with ice-cold PBS and irradiated with 0.15 J/cm^2 of 365-nm UV light at 4°C. The cells were collected by centrifugation at 514 × *g* for 1 min at 4°C. The cell pellets were resuspended in cross-linking and immunoprecipitation (CLIP) lysis buffer supplemented with protease inhibitors (Roche) and 0.5 U/μl RNasin (Promega) and sonicated twice with 10-s bursts (30). The lysates were mixed with 10 μl of a 1:250 dilution of RNase I (Life Technologies) and 2 μl of Turbo DNase (Life Technologies) with shaking at 37°C for 3 min. The lysates were then cleared and immunoprecipitated with 2 μg of anti-Sam68 or anti-SRSF1 antibody and control mouse/rabbit IgGs (Santa Cruz). Proteinase K buffer (containing 1.2 mg/ml proteinase K) was added to the immunoprecipitates and incubated for 20 min at 37°C. RNA was isolated through TRIzol reagent and subjected to RT-qPCR. The reverse primers listed below were used for the reverse transcription reaction. qPCR was performed with the following primers for *Rps6kb1*: intron 6 SBS, 5′-GAT TCA GGT CAT GAT TCA TG-3′ (forward) and 5′-CAG TGG GAA GGT GGT TTT GC-3′ (reverse); exon 6 (SRSF1 site), 5′-GAG GAG AAC TAT TTA TGC AG-3′ (forward) and 5′-GAA TAT TCC CTC TCT TTC TAA-3′ (reverse); exon 7, 5′-TTT ACT TGG CTG AAA TCT CC-3′ (forward) and 5′-CTT GGT GAT TAA GCA TGA TG-3′ (reverse).

RESULTS

Sam68 regulates the alternative splicing of *Rps6kb1* in preadipocytes and mouse white adipose tissue (WAT). Sam68-deficient preadipocytes are unable to differentiate into mature adipocytes (16). We reported that Sam68-deficient preadipocytes have decreased mTOR expression as they increase the production of a short mTOR$_{i5}$ isoform rather than synthesizing the full-length mTOR mRNA (16). The Sam68-deficient preadipocyte defect is partially rescued by the ectopic expression of the full-length mTOR expression, suggesting that there may be other splicing events regulated by Sam68 in the mTOR signaling pathway. To identify these alternative splicing events that contribute to the differentiation defects of Sam68-deficient preadipocytes, we monitored the presence of spliced isoforms in the mTOR signaling pathway. Using the Ensembl database, we identified the existence of spliced isoforms for the murine *Rps6kb1*, *TSC1*, *Rheb*, *Akt1*, and *Deptor* genes but not for *IRS1*, *TSC2*, *4EBP1*, or *eIF4E*. Among the candidate isoforms tested, we observed that the mRNA levels of isoform *Rps6kb1-002* were dramatically increased in Sam68-deficient cells (Sam68sh) (Fig. 1A) compared to levels in control pRetrosuper 3T3-L1 cells (Fig. 1B). We also noted a slight to moderate upregulation of isoforms *TSC1-003*, *Rheb-003*, *Akt1-003*, and *Rps6kb1-005* in Sam68sh 3T3-L1 cells, and we did not observe significant fluctuations with the following isoforms in Sam68sh 3T3-L1 cells: *TSC1-006*, *Rheb-002*, and *Deptor-002* (see Fig. S1 in the supplemental material).

We next examined the levels of isoform *Rps6kb1-002* in white adipose tissue (WAT) of wild-type and Sam68 null mice. The level of *Rps6kb1-002* was more abundant in white adipose tissue of Sam68 deficient mice than in the tissue of the littermate control mice (Fig. 1C). The increase in the mRNA ratio of *Rps6kb1-002 to Rps6kb1* was also confirmed by RT-qPCR in Sam68-deficient preadipocytes and WAT isolated from Sam68 null mice (Fig. 1D). Thus, the loss of Sam68 promotes the production of splicing variant *Rps6kb1-002*.

Sam68 deficiency increases the expression of p31S6K1. *Rps6kb1* encodes p85/p70 S6K1, and the inclusion of alternative exons 6a, 6b, and 6c leads to the generation of the *Rps6kb1-002* isoform (Fig. 1E). The *Rps6kb1* transcript generates two proteins due to alternative mRNA translation start sites resulting in p70S6K1 and p85S6K1, whereas the shorter *Rps6kb1-002* isoform harbors only the first six exons with alternative exons 6a, 6b, and 6c; and its alternative splicing was shown to be positively regulated by SRSF1 (31). The presence of a stop codon in exon 6c generates a truncated protein of 31 kDa, termed p31 or p31S6K1, that expresses the S6K1 N-terminal domain followed by a truncated kinase domain. The increase of *Rps6kb1-002* mRNA was reflected at the protein level since we observed the presence of p31S6K1, as well as p70S6K1, in Sam68-deficient preadipocytes by immunoblotting with an N-terminal S6K1 antibody (BD Transduction Lab, Inc.) (Fig. 2A). We observed similar results in mouse WAT isolated from Sam68$^{-/-}$ mice using a different anti-S6K1 antibody (Cell Signaling, Inc.) that detects p31S6K1 in addition to p70S6K1 and p85S6K1 (Fig. 2B). As SRSF1 is a known regulator of p31S6K1 (31) and as Sam68 has been shown to regulate the alternative splicing of *Srsf1* associated with nonsense-mediated decay (9), we performed immunoblotting to examine SRSF1 levels in the absence of Sam68. The depletion of Sam68 in preadipocytes or Sam68-deficient WAT did not affect the SRSF1 protein levels (Fig. 2A and B). These findings show that Sam68-deficient preadipocytes have increased p31S6K1 expression using two different N-terminal S6K1 antibodies with little to no effect on the global expression of p70S6K1, p85S6K1, and SRSF1.

Sam68 binds an RNA element within intron 6 that diminishes SRSF1 binding to *Rps6kb1* exon 6. Sam68 binds RNA with U(U/A)AA motifs with high affinity (3, 4). Sam68 binding sites

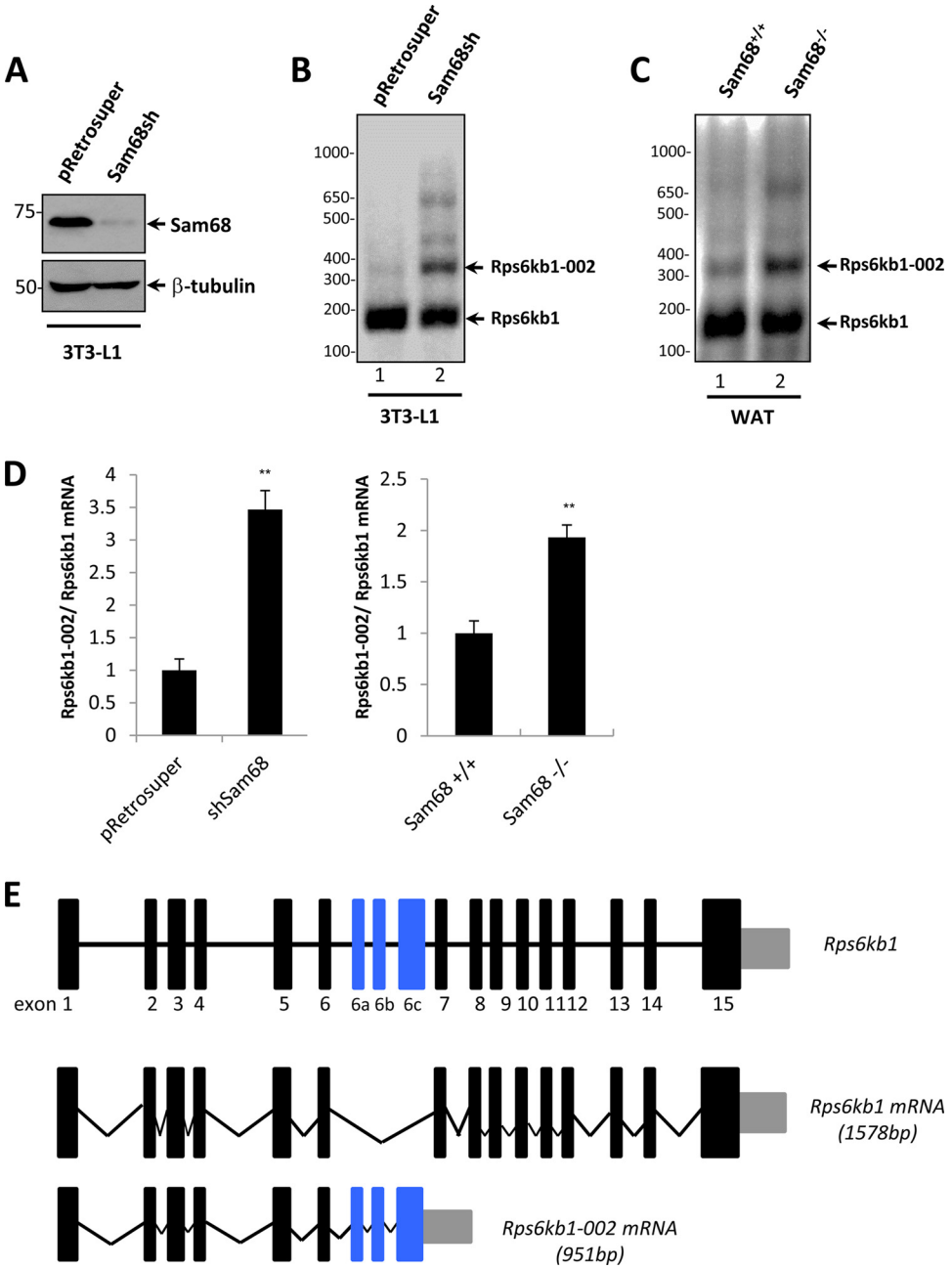

FIG 1 Sam68 regulates the alternative splicing of *Rps6kb1* in mouse preadipocytes and WAT. (A) Mouse 3T3-L1 preadipocytes stably transfected with pRetrosuper or Sam68sh pRetrosuper were lysed and immunoblotted with anti-Sam68 and anti-β-tubulin antibodies. The molecular mass markers are shown on the left in kilodaltons. (B and C) Total RNA from undifferentiated pRetrosuper and Sam68sh 3T3-L1 cells and mouse WAT was isolated and analyzed using a three-primer RT-PCR strategy with a common forward primer in exon 5 and reverse primers in exons 6 and 6b. The DNA markers are shown on the left in base pairs. (D) Total RNA from pRetrosuper and Sam68sh 3T3-L1 cells and mouse WAT was isolated and subjected to RT-qPCR. The presence of *Rps6kb1-002* is expressed as a ratio of total *Rps6kb1* transcripts. Error bars represent standard deviations of the means (**, $P < 0.01$). (E) Schematic representation of *Rps6kb1* gene, the wild-type isoform *Rps6kb1*, and alternative spliced isoform *Rps6kb1-002*. Constitutive exons are shown as black boxes, and alternative exons are shown in blue. Introns are shown as horizontal lines, and splicing events are indicated by angled lines. The 3′ UTRs are shown as gray boxes.

(SBSs) often reside near splice sites within pre-mRNAs, acting either as splice enhancers or silencers to regulate neighboring splice site usage (1). Since the absence of Sam68 increases the splicing of *Rps6kb1-002*, we searched intron 6 for repeats of the U(U/A)AA motif. The *Rps6kb1* gene sequence is shown in Fig. 3A with the *Rps6kb1-002* alternative exons in blue. We identified a putative Sam68 binding site within *Rps6kb1* intron 6 with an encoded sequence of 5′-UAAUUAAA-3′, termed the SBS, 68 nucleotides downstream of a putative SRSF1 binding site in exon 6 (Fig. 3A). To determine whether Sam68 binds the SBS sequence, we synthesized a biotinylated RNA of the SBS, as well as a biotinylated control RNA (SBSmut) that has the 5′-UAAUUAAA-3′ sequence

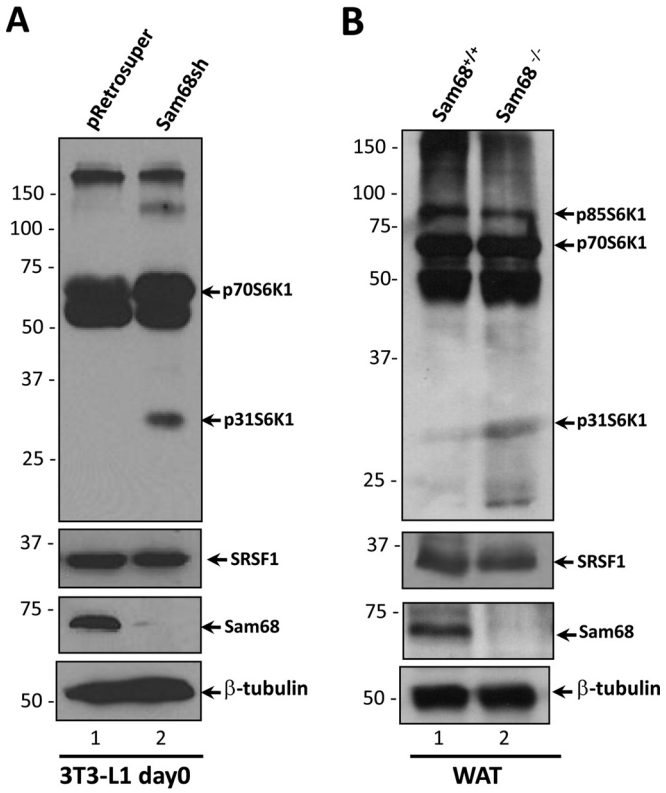

FIG 2 Sam68 regulates the expression of p31S6K1 but not that of SRSF1 in preadipocytes and WAT. Protein extracts from pRetrosuper and Sam68sh 3T3-L1 cells or from mouse WAT were immunoblotted with anti-S6K1 antibodies from BD Transduction Labs (A) or Cell Signaling, Inc. (B). Anti-Sam68 and anti-β-tubulin antibodies were used to monitor the levels of Sam68 and β-tubulin, respectively. Molecular mass markers are shown on the left in kilodaltons.

replaced with 5′-UAAUUCCA-3′ (substitutions are underlined) (Fig. 3B). The RNA oligonucleotides harboring either a wild-type or mutated SBS were used to perform affinity pulldown assays. Cell lysates from undifferentiated wild-type 3T3-L1 cells were incubated with the biotinylated RNAs, and complexes were purified with streptavidin-Sepharose beads. The bound proteins were separated by SDS-PAGE and immunoblotted for Sam68. Wild-type SBS bound Sam68 with a much higher affinity than the mutated SBS, as assessed by increasing the concentration of salt in the wash buffer (Fig. 3B). These findings show that Sam68 associates *in vitro* with RNA sequences within intron 6 of the *Rps6kb1* pre-mRNA.

We next examined whether endogenous Sam68 bound the intron 6 SBS *in vivo* using UV cross-linking and immunoprecipitation (CLIP) with a dilution of RNase I (1:250) that digests RNAs into fragments of 50 to 300 nucleotides in length (30). Preadipocytes (pRetrosuper and Sam68sh cells) were prepared for CLIP, as described in Materials and Methods, and immunoprecipitated with either control immunoglobulin G (IgG), anti-Sam68 antibodies, or anti-SRSF1 antibodies. The putative binding sites were mapped by using the primers indicated in Fig. 4A. Anti-Sam68 immunoprecipitations compared to those with IgG were enriched ~25-fold for the *Rps6kb1* intron 6 region spanning the SBS but not for an RNA region spanning *Rps6kb1* exon 7 in pRetrosuper 3T3-L1 cells (Fig. 4B). In contrast, there was no RNA enrichment detected in anti-Sam68 immunoprecipitations in Sam68sh 3T3-L1 cells, as expected (Fig. 4B). These findings suggest that Sam68 associates *in vivo* with the SBS site of the *Rps6kb1* intron 6. CLIP with anti-SRSF1 antibodies revealed a modest 2-fold enrichment of the *Rps6kb1* exon 6 fragment encompassing the putative SRSF1 binding site over levels in control in pRetrosuper 3T3-L1 cells (Fig. 4C). Interestingly, cells depleted of Sam68 contained an ~6-fold increase in SRSF1 at this site (Fig. 4C), suggesting that Sam68 occupancy at the SBS prevents SRSF1 binding to exon 6. Taken together, these data suggest that Sam68 directly associates with the SBS and that the presence of Sam68 influences SRSF1 binding to exon 6.

Sam68 and SRSF1 are known to interact as endogenous Sam68 immunoprecipitations contain SRSF1, as detected by mass spectrometry analysis (32). To confirm the interaction, HEK293 cells were cotransfected with GFP-Sam68 and GFP-SRSF1. The cells were lysed and immunoprecipitated with control IgG or anti-SRSF1 antibodies. The bound proteins were separated by SDS-PAGE and immunoblotted with anti-Sam68 antibodies. Both GFP-Sam68 and endogenous Sam68 coimmunoprecipitated with SRSF1 but not with control IgG (Fig. 4D, upper panel). Immunoblotting with anti-SRSF1 antibodies confirmed that GFP-SRSF1 and endogenous SRSF1 were immunoprecipitated (Fig. 4D, lower panel). These data confirm that Sam68 interacts with SRSF1.

Minigene assays indicate that Sam68 suppresses the alternative splicing of *Rps6kb1-002*. A splicing minigene was constructed with a cytomegalovirus (CMV) promoter driving the expression of a 1.6-kb genomic fragment encompassing *Rps6kb1* exon 6, intron 6, and exon 7 (Fig. 5A). The minigene transcription start site was located in the plasmid upstream of *Rps6kb1* exon 6, followed by the sequence of a FLAG epitope tag. A forward primer complementary to the FLAG cDNA sequence (F1) and reverse primers in exons 6c (R1), exon 6a (R3), and 7 (R2 and R4) recognize fragments corresponding to *Rps6kb1-002* and *Rps6kb1*, respectively. pRetrosuper and Sam68sh 3T3-L1 cells were transfected with either pcDNA3.1, the wild-type *Rps6kb1*, or the SBS mutated (SBSmut) minigene. Total RNA was isolated 48 h after transfection, treated with RQ1 DNase, and monitored for *Rps6kb1-002* and *Rps6kb1* transcripts using three-primer RT-PCR (Fig. 5B) and RT-qPCR (Fig. 5C). There was little expression of the *Rps6kb1-002* fragment from the wild-type minigene in pRetrosuper cells (Fig. 5B, lane 2); however, the presence of the *Rps6kb1-002* transcript increased (~6- to 8-fold) when the SBS was mutated or when Sam68 was ablated in the cells (Fig. 5B, lanes 3 and 5, and C). Interestingly, the deletion of the SBS in addition to the ablation of Sam68 in 3T3-L1 cells led to an ~40-fold increase in the *Rps6kb1-002* transcript (Fig. 5B, lane 6, and C). These findings show that Sam68 and the SBS negatively regulate *Rps6kb1-002*.

We next overexpressed Sam68 to examine its influence on the wild-type and SBSmut *Rps6kb1* minigenes. The expression of GFP-Sam68 in HEK293 cells was confirmed by immunoblotting (Fig. 5D). Mutation of the SBS led to an increase in *Rps6kb1-002* in control pcDNA3.1-transfected cells (Fig. 5E). However, the expression of GFP-Sam68 completely quenched the expression of *Rps6kb1-002* production from both minigenes (Fig. 5E). These findings suggest that Sam68 is a potent repressor of *Rps6kb1-002* and also has SBS-independent functions.

Sam68 counteracts the positive effects of SRSF1 for *Rps6kb1-002* expression. We next confirmed that SRSF1 was responsible for regulating the p31S6K1 levels in Sam68sh 3T3-L1 cells. Deple-

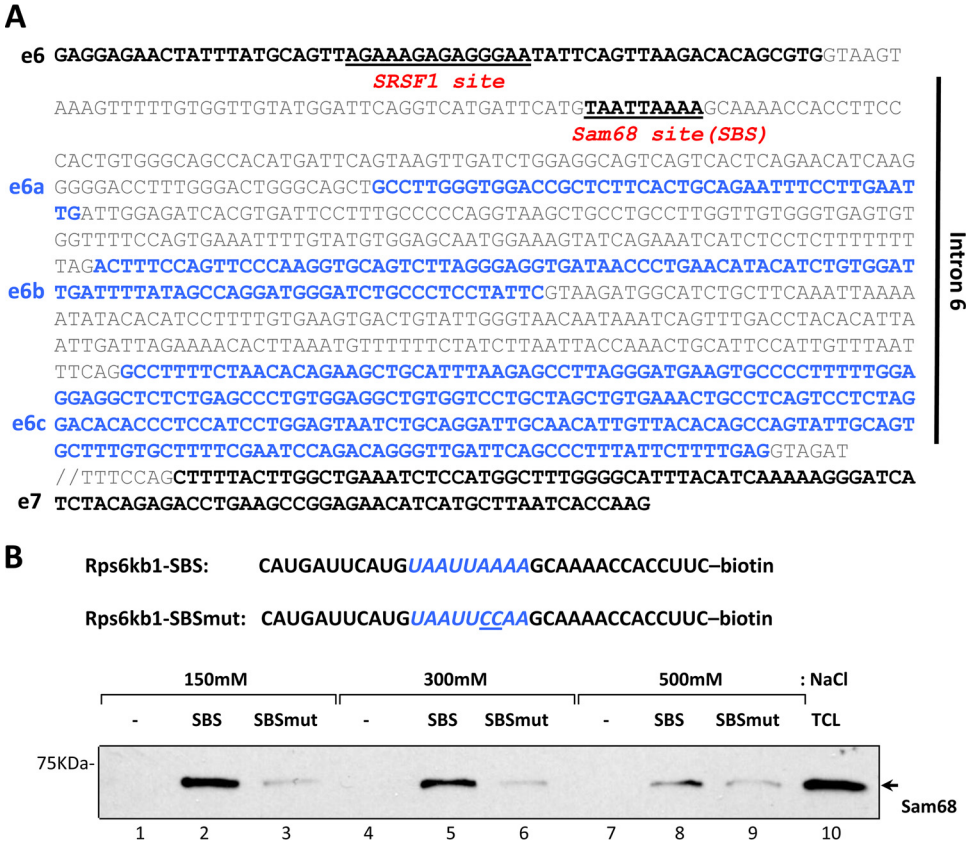

FIG 3 Sam68 associates *in vitro* with RNA elements in *Rps6kb1* intron 6. (A) Sequence spanning mouse *Rps6kb1* exon 6, intron 6, which contains the three alternative exons (6a, 6b, and 6c) and exon 7, taken from the Ensembl browser. Underlined sequences represent the Sam68 binding site (SBS) within intron 6 and the SRSF1 binding site in exon 6. (B) The sequences of intron 6 and SBS and of the mutated version (SBSmut) of the synthetic RNAs generated. Affinity pulldown assays were performed with biotinylated RNA and streptavidin beads using 3T3-L1 cells and immunoblotted with anti-Sam68 antibodies. TCL, total cell lysate. A molecular mass marker is shown on the left.

tion of SRSF1 using siRNA reduced the levels of p31S6K1 protein (Fig. 6A) and decreased *Rps6kb1-002* mRNA in Sam68sh but not pRetrosuper 3T3-L1 cells, as assessed by RT-qPCR (Fig. 6B). These findings confirm that SRSF1 is required for the production of *Rps6kb1-002* in adipocytes.

To examine the influence of SRSF1 and Sam68 on the alternative splicing of *Rps6kb1*, we transfected the *Rps6kb1* minigenes in HEK293 cells. SRSF1 was efficiently depleted using siRNAs in these cells (Fig. 7A). The presence of the *Rps6kb1-002* isoform was increased with the mutation of the SBS in siGFP-transfected but not siSRSF1-transfected HEK293 cells (Fig. 7B). These findings suggest that SRSF1 is a positive regulator of *Rps6kb1-002*. We next cotransfected GFP-SRSF1 and GFP-Sam68 in HEK293 cells and assayed for the presence of the *Rps6kb1-002* transcript generated from the wild-type *Rps6kb1* minigene (Fig. 7C and D). GFP-SRSF1 increased the appearance of *Rps6kb1-002* in a dose-dependent manner (Fig. 7D), and this increase was attenuated with the overexpression of GFP-Sam68 (Fig. 7D, lanes 5 to 8). These data show that Sam68 counteracts the positive effects of SRSF1 in regulating the production of *Rps6kb1-002*.

The ectopic expression of p31S6K1 suppresses adipogenesis. The direct role of *Rps6kb1-002* in adipogenesis was investigated. Preadipocytes were stably transfected with pcDNA3.1 (control) or an expression vector encoding FLAG-p31S6K1. Two stable clones (FLAG-p31 clones 3 and 10) ectopically expressing p31S6K1 were selected (Fig. 8A), and their expression was comparable to levels observed in Sam68-deficient cells (data not shown). p31S6K1-expressing cells were monitored for lipid accumulation following differentiation for 4 days. We observed a notable decrease of lipid accumulation in both p31S6K1-overexpressing 3T3-L1 cell lines compared to levels in control cells, as visualized by Oil Red O staining (Fig. 8B). We subsequently examined the expression pattern of adipose-specific markers at differentiation day 0 and day 4 (Fig. 8C). The mRNA levels of PPARγ, C/EBPα, and GLUT4 were increased dramatically in control cells (pcDNA3.1) upon differentiation, as expected, while in clones 3 and 10, the expression of these markers was largely absent after differentiation day 4 (Fig. 8C). These results show that p31S6K1 is a repressor of adipogenesis.

Depletion of p31S6K1 in Sam68-deficient preadipocytes partially rescues the adipogenesis defect. We examined whether the elevated level of p31S6K1 is a contributing factor for the adipogenesis defect of Sam68-deficient 3T3-L1 cells. To test this possibility, we decreased the expression of p31S6K1 using siRNA specific to this isoform. pRetrosuper and Sam68sh 3T3-L1 cells were transfected with either siGFP or two different p31S6K1 siRNAs, designated sip31-A and sip31-B. The elevated expression of p31S6K1 in Sam68sh 3T3-L1 cells was depleted in sip31-A- and

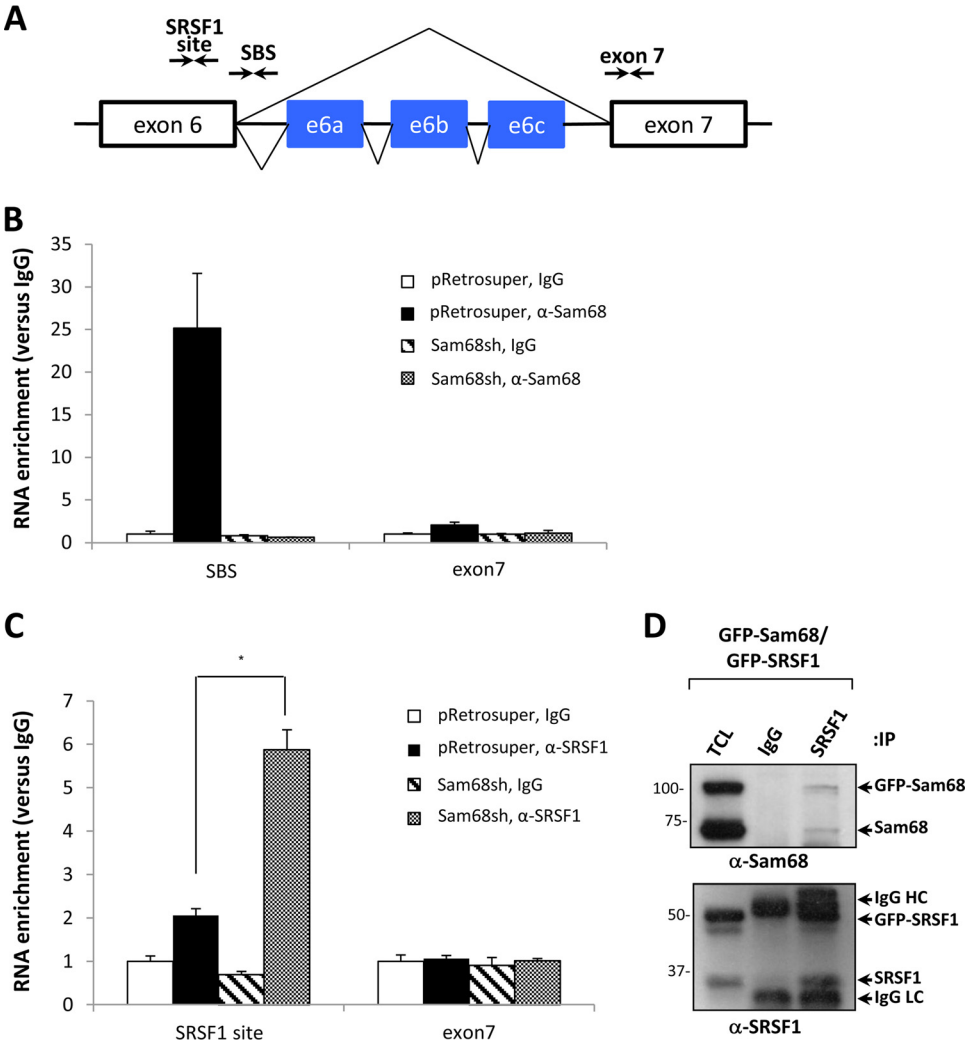

FIG 4 Sam68 binds an intronic SBS and prevents the binding of SRSF1 to its consensus site in *Rps6kb1* exon 6. (A) Schematic of the genomic architecture of *Rps6kb1* spanning exons 6 and 7 with three alternative exons located in intron 6. Arrows depict the primer pairs used in RT-qPCR to detect the RNA-bound Sam68 binding site (SBS), the exon 6 SRSF1 binding site, and exon 7 as a negative control. (B and C) CLIP assays were performed using anti-Sam68 antibodies and anti-SRSF1 antibodies or control IgGs. Bound RNA was analyzed in triplicate by RT-qPCR with the primers shown in panel A. The levels of bound RNA of the SBS, SRSF1 binding site, and exon 7 in immunoprecipitates were normalized to the levels of the total RNA in the input. Mean values are expressed as fold enrichment. Error bars represent standard deviations of the means (*, $P < 0.05$). (D) HEK293 cells were transfected with expression vectors encoding GFP-Sam68 and GFP-SRSF1. After 48 h, the cells were lysed and subjected to immunoprecipitation (IP) and immunoblotting. The migration of GFP-Sam68, Sam68, GFP-SRSF1, SRSF1, and the heavy chain (HC) and light chains (LC) of IgG is indicated. TCL, total cell lysate. Molecular mass markers are shown on the left in kilodaltons.

sip31-B-transfected cells (Fig. 9A). Sam68sh 3T3-L1 cells exhibited reduced adipogenesis compared to levels in pRetrosuper cells, as previously reported (16), and the presence of transfected siGFP had no influence on adipogenesis as visualized by Oil Red O staining (Fig. 9B). The transfection of p31S6K1 siRNA increased lipid accumulation in Sam68-deficient cells, suggesting that the loss of p31S6K1 expression partially rescues the adipogenesis defect observed in Sam68sh cells (Fig. 9B, compare staining of siGFP with that of sip31-A and sip31-B). We also examined the expression pattern of adipose-specific markers at differentiation days 0 and 4 of 3T3-L1 cells. The mRNA levels of PPARγ, C/EBPα, and GLUT4 were increased in pRetrosuper cells upon differentiation, as expected (Fig. 9C). Strikingly, the attenuated expression of differentiation markers (PPARγ, C/EBPα, and GLUT4) in Sam68sh cells was partially derepressed with the depletion of p31S6K1 (Fig. 9C). These results indicate that expression of p31S6K1 represses adipogenesis and is a contributing factor for the observed defects in Sam68-deficient preadipocytes.

To answer the question of whether there was a specific change in the levels of the *Rps6kb1-002* isoform or just a general change in the expression levels of the whole gene (including both isoforms) that contributes to adipogenesis, we abrogated total S6K1 expression using siRNAs. pRetrosuper 3T3-L1 cells were transfected with either siGFP or siRNA targeting both p70/p31 S6K1 isoforms (Fig. 10A). Deletion of total S6K1 in pRetrosuper 3T3-L1 cells had no influence on adipogenesis as cells differentiated normally (Fig. 10B) and expressed high levels of PPARγ, C/EBPα, and GLUT4 at day 4 of differentiation (Fig. 10C). Since p31S6K1 is absent in

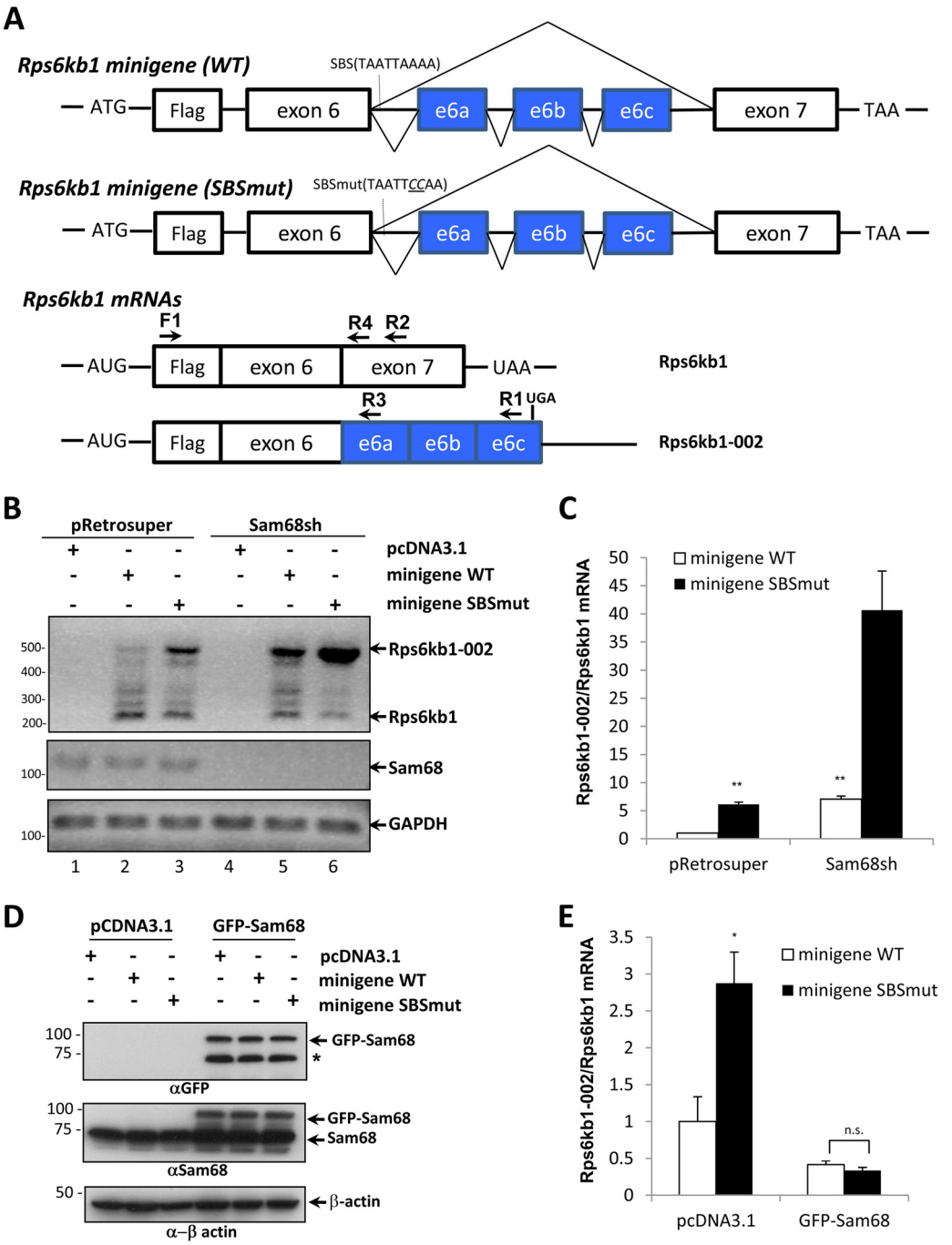

FIG 5 *Rps6kb1* minigene assay defines intron 6 as the minimal requirement. (A) Mouse genomic fragment encompassing *Rps6kb1* exons 6 and 7 was cloned in pcDNA3.1 with an N-terminal FLAG epitope tag. The SBS is shown in the proximity of the 5′ splice site within intron 6. The same mouse genomic fragment containing CC replacing AA in the Sam68 binding site was also constructed in pcDNA3.1 with an N-terminal FLAG epitope tag. The splicing of the wild-type *Rps6kb1* and SBSmut *Rps6kb1* minigenes leads to two different transcripts. Arrows indicate the primers used in the minigene assay. (B and C) pRetrosuper and Sam68sh 3T3-L1 cells were transfected with either pcDNA3.1 alone, *Rps6kb1* (WT), or the *Rps6kb1* (SBSmut) minigene. Total RNA was isolated and digested with RQ1 DNase, and the levels of *Rps6kb1-002* and *Rps6kb1* transcripts were assessed by semiquantitative RT-PCR using primer F1 with R1 and R2 (B) or by RT-qPCR using F1 with R3 and R4 (C). In panel B the mRNA levels of Sam68 and GAPDH were also assessed. Error bars represent standard deviations of the means (**, $P < 0.01$). (D) HEK293 cells were cotransfected with either pcDNA3.1 or GFP-Sam68 alone with the *Rps6kb1* minigene or *Rps6kb1* minigene SBSmut. The cells were harvested after 48 h, and the cellular extracts were immunoblotted with anti-GFP, anti-Sam68, and anti-β-actin antibodies. The asterisk denotes a nonspecific protein recognized with anti-GFP antibodies. (E) The total RNA from the cells indicated in panel D was isolated and treated with RQ1 DNase, and the mRNA levels of *Rps6kb1* and *Rps6kb1-002* were assessed by RT-qPCR. The mRNA expression level of *Rps6kb1-002* was normalized to *Rps6kb1* levels. Error bars represent standard deviations of the means (*, $P < 0.05$; n.s., not significant).

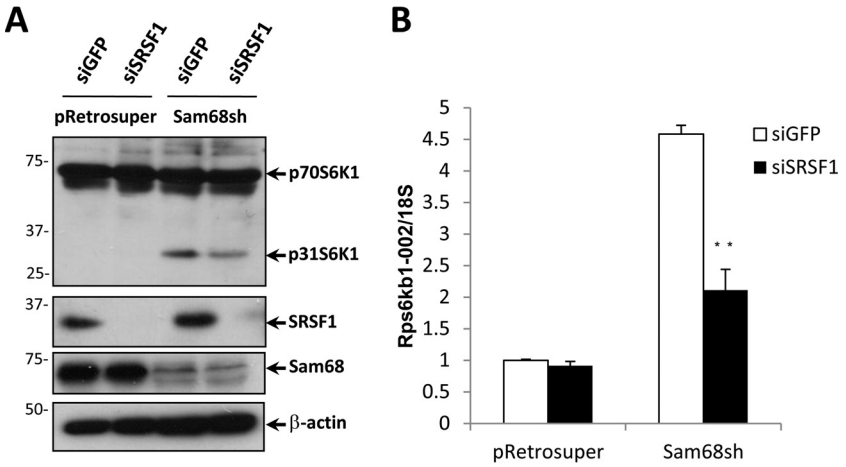

FIG 6 The presence of the *Rps6kb1-002* isoform in Sam68-depleted preadipocytes requires SRSF1. (A) pRetrosuper or Sam68sh 3T3-L1 cells were transfected with siGFP or siSRSF1. The protein extracts were prepared 48 h after and immunoblotted with the indicated antibodies. β-Actin is shown as the loading control. Molecular mass markers are shown on the left in kilodaltons. (B) The total RNA was isolated from pRetrosuper or Sam68sh 3T3-L1 cells transfected with siGFP or siSRSF1. The mRNA levels of *Rps6kb1-002* were assessed by RT-qPCR and normalized to the level of 18S rRNA. Error bars represent standard deviations of the means (**, $P < 0.01$).

pRetrosuper cells, these findings demonstrate that deletion of p70S6K1 alone does not affect 3T3-L1 differentiation, as reported previously (27). Next, we examined whether Sam68sh 3T3-L1 cells were partially rescued with siRNAs targeting p70/p31S6K1, and indeed this was the case (Fig. 10B and C). The partial derepression we observed was similar to decreasing the levels of p31S6K1 alone (compare Fig. 9 and 10). These observations indicate that p31S6K1 inhibits adipogenesis independent of the p70S6K1 isoform.

DISCUSSION

Alternative splicing leads to the generation of key isoforms required for cellular differentiation and proliferation (33). In the present manuscript, we report that the Sam68 RNA binding protein exerts a suppressive effect on the alternative splicing of the ribosomal S6 kinase gene (*Rps6kb1*) in adipocytes. Consequently, Sam68-depleted 3T3-L1 preadipocytes harbor elevated levels of the short isoform 2 of S6K1 (*Rps6kb1-002*) and its encoded protein p31S6K1. Mechanistically, Sam68 binds an RNA element (Sam68 binding site, SBS) in intron 6 near the 5′ splice site and prevents the usage of alternative exons 6a, 6b, and 6c that generate *Rps6kb1-002* by counteracting the positive effects of the serine/arginine-rich splicing factor 1 (SRSF1) that binds within exon 6. The ectopic expression of p31S6K1 in wild-type preadipocytes inhibited adipogenesis, and the depletion of p31S6K1 using two separate siRNAs partially restored the adipogenesis defects in Sam68-deficient preadipocytes. These findings demonstrate that the expression of Sam68 in adipocytes is required to prevent the expression of the short isoform 2 of S6K1, a potent suppressor of adipogenesis.

We identified an A/U-rich intronic sequence bound by Sam68, 46 nucleotides downstream of the 5′ splice site of *Rps6kb1* exon 6. Deletion of this element promoted the skipping of *Rps6kb1* exons 6a, 6b, and 6c, thus preventing the expression of *Rps6kb1-002*. Sam68 is an established regulator of alternative splicing, and it is known to function by directly associating with A/U-rich elements near 5′ splice sites (5, 10, 12, 16). The *Rps6kb1* intron 6 UAAU UAAA bipartite sequence is recognized by Sam68 with relatively high affinity. Mutation of the SBS to UAAUUCCA (mutated residues underlined) diminished Sam68 association with this RNA sequence. By performing CLIP assays, we confirmed that Sam68 localizes directly at the SBS *in vivo* as anti-Sam68 immunoprecipitations enriched the SBS RNA sequence 25-fold over levels of control immunoprecipitations (Fig. 4B). The presence of Sam68 suppressed the positive effects of SRSF1 on the production of *Rps6kb1-002*, as measured using a minigene. SRSF1 is a known positive regulator of *Rps6kb1-002* (31), but its *Rps6kb1* binding site(s) and how it regulates the production of *Rps6kb1-002* remained unknown. We show that SRSF1 displayed reduced binding to its *Rps6kb1* exon 6 GAAAGAGAGGGAA site in the presence of Sam68 by CLIP assays. Using the *Rps6kb1* minigene, mutation of the SBS increased *Rps6kb1-002* production, and the increase was observed in the presence or absence of Sam68 (knockdown cells), suggesting that the SBS also has Sam68-independent functions. It is possible that the residual Sam68 levels in the knockdown cells play this role or that the SBS is scavenged by other A/U-rich RNA binding repressors in the absence of Sam68. Alternatively, the SBS may regulate local RNA secondary structure that influences *Rps6kb1-002* alternative splicing by SRSF1.

Several possible mechanisms have been proposed to explain how RNA binding proteins suppress neighboring SR proteins (33–35). Sam68 could compete directly with SRSF1 for the splicing machinery for intron 6 definition. Sam68 may also alter the neighboring RNA secondary structure and/or the rate of transcription, as proposed by Batsche and coworkers (36). The rate of transcription may influence the binding of SRSF1, thus influencing exon selection (33–35).

We show that *Rps6kb1-002* and its encoded protein, p31S6K1, are present in Sam68-depleted preadipocytes and mouse white adipose tissue of Sam68 null mice. Sam68 protein expression increases during adipogenesis (16), and its role may be, in part, to ensure the suppression of *Rps6kb1-002*. Using an anti-S6K1 antibody that recognizes all the isoforms sharing the common N terminus, we observed that Sam68 deficiency leads

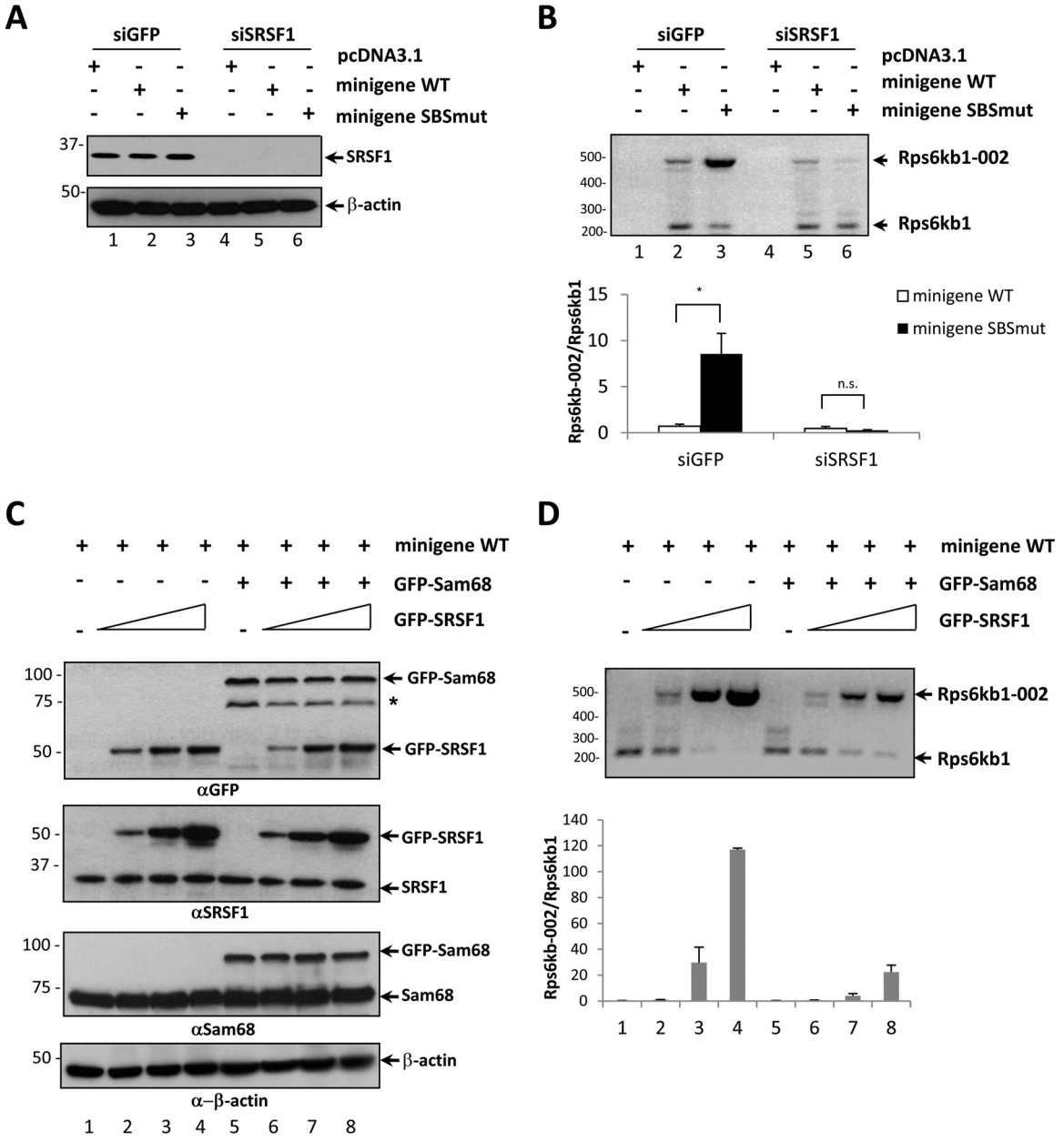

FIG 7 Sam68 competes with SRSF1 for the positive regulation of *Rps6kb1* splicing. (A) HEK293 cells were transfected with siRNAs targeting either GFP or human SRSF1. After 24 h, cells were transfected with either pcDNA3.1, the *Rps6kb1* wild-type minigene plasmid, or the *Rps6kb1* SBSmut minigene plasmid. The cells were harvested after 48 h. Protein extracts were immunoblotted with the indicated antibodies. β-Actin is shown as the loading control, and the asterisk denotes an unknown protein. Molecular mass markers are shown on the left in kilodaltons. (B) Total RNA was isolated and treated with RQ1 DNase, and the mRNA levels of *Rps6kb1* and *Rps6kb1-002* were assessed by RT-PCR using the primer pairs indicated in Fig. 5A. Densitometry analysis was performed from two independent experiments, and fold induction of *Rps6kb1-002* was normalized to the level of *Rps6kb1*. Error bars represent standard deviations of the means (*, $P < 0.05$; n.s., not significant). (C) HEK293 cells were cotransfected with either the *Rps6kb1* minigene plasmid alone or with GFP-Sam68 or with increasing amounts of GFP-SRSF1. The cells were harvested after 48 h. The protein extracts were immunoblotted with the indicated antibodies. β-Actin is shown as the loading control. (D) Total RNA was isolated and treated with RQ1 DNase, and the mRNA levels of *Rps6kb1* and *Rps6kb1-002* were assessed by RT-PCR. Densitometry analysis was performed from two independent experiments, and fold induction of *Rps6kb1-002* was normalized to the level of *Rps6kb1*. Error bars represent standard deviations of the means.

to increased p31S6K1 expression, without the apparent reduction in p70S6K1 and p85S6K1 expression. The latter is probably due to the fact that p70/p85 S6K1 are considerably more abundant than p31S6K1 (31). The cellular role of p31S6K1 is unknown; however, it does have oncogenic properties. The expression of p31S6K1 is sufficient to induce transformation in NIH 3T3 cells (31). Unlike mice, which express only one short isoform, humans generate two short isoforms (h6A and h6C) of S6K1, and their expression is elevated in breast cancer cell lines (37). Depletion of these isoforms in breast cancer cell lines decreases their proliferation (37). These short isoforms lack kinase activity because their kinase domains are truncated;

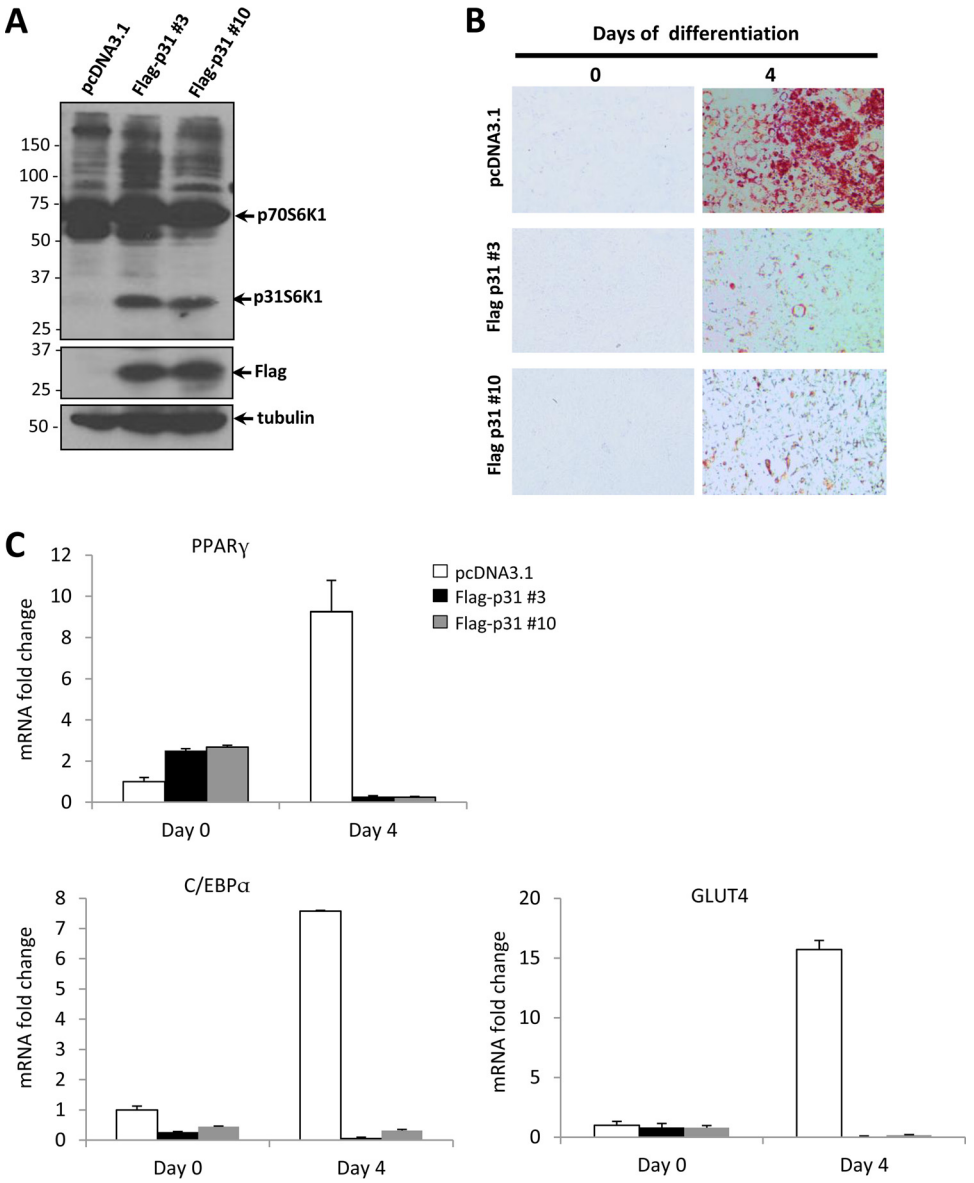

FIG 8 Ectopic expression of p31S6K1 suppresses adipogenesis. (A) 3T3-L1 cells were stably transfected with pcDNA3.1 or FLAG-p31S6K1. A polyclonal population of pcDNA3.1 and two individual clones (FLAG-p31 3 and FLAG-p31 10) was selected for analysis by immunoblotting using the indicated antibodies. β-Tubulin is shown as the loading control. Molecular mass markers are shown on the left in kilodaltons. (B) The cells indicated in panel A were induced to differentiate for 4 days. Adipocyte differentiation was assessed by Oil Red O staining. (C) The mRNA levels of PPARγ, C/EBPα, and GLUT4 normalized to 18S rRNA were assessed by RT-qPCR. The data are expressed as relative values from differentiation days 0 and 4. Error bars represent standard deviations of the means.

however, they retain the ability to bind mTORC1 as they contain the Raptor binding motif (38). p31S6K1 has been shown to associate with mTOR and increase its activity (37); however, this activity in Sam68-deficient preadipocytes is difficult to assess since these cells have reduced mTOR levels (16). Indeed, Sam68-deficient preadipocytes exhibit decreased phosphorylation of rpS6 and AKT during adipogenesis (16). p31S6K1 has also been shown to be nuclear, unlike p85S6K1 and p70S6K1 (39); therefore, it may also fulfill other functions.

S6K1$^{-/-}$ mice have decreased adipose tissue mass, increased energy expenditure, and are resistant to dietary-induced obesity (40). S6K1 participates in the upregulation of transcription factors during the commitment phase of adipogenesis (27). Adipocytes normally express p70/p85S6K1 but not p31S6K1 (Fig. 2). The expression of p31S6K1 in 3T3-L1 cells prevented adipogenesis. Depletion of both p70S6K1 and p31S6K1 rescued the adipogenesis defects of Sam68-deficient cells to a similar extent as depletion of p31S6K1 alone, indicating that the negative effects of p31S6K1 in adipogenesis are independent of p70S6K1. Therefore, p31S6K1 contributes to the Sam68 deficiency-induced adipogenesis defects observed.

Sam68 likely regulates many alternative spliced events that contribute to the observed lean phenotype of Sam68-deficient mice (16). Sam68 regulates the splicing of Bcl-x (8), as well as mTOR, tripeptidyl peptidase II (Tpp2), and Tubby (Tub) (16).

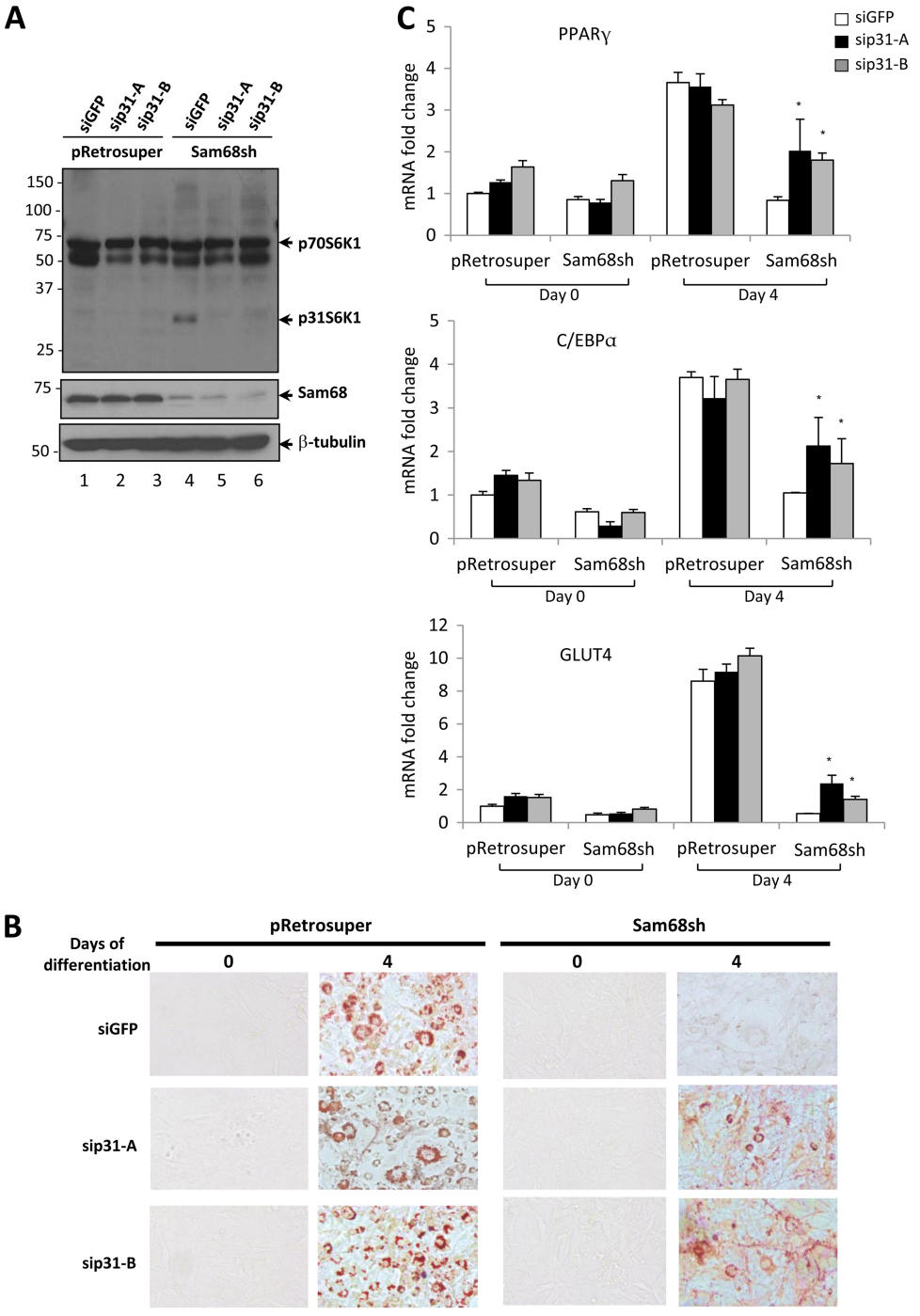

FIG 9 The expression of p31S6K1 contributes to the adipogenesis defects of Sam68-deficient mouse preadipocytes. (A) pRetrosuper or Sam68sh 3T3-L1 cells were transfected with siGFP (control), sip31-A, and sip31-B. The protein extracts were immunoblotted with the indicated antibodies. β-Tubulin is shown as the loading control. Molecular mass markers are shown on the left in kilodaltons. (B) The cells indicated in panel A were induced to differentiate for 4 days. Adipocyte differentiation was assessed by Oil Red O staining. (C) The mRNA levels of PPARγ, C/EBPα, and GLUT4 normalized to GAPDH were assessed by RT-qPCR. The data are expressed as relative values from differentiation days 0 and 4. Error bars represent standard deviations of the means (*, $P < 0.05$).

Sam68 has also been shown to regulate the alternative splicing of the *Srsf1* transcript in colon cancer cells to influence the epithelial-to-mesenchymal transition (9). Indeed, we also detected an increase in the *Srsf1* NMD transcript in 3T3-L1 cells (data not shown), but this did not affect SRSF1 protein levels.

In conclusion, we show that the alternative splicing of the mouse *Rps6kb1* gene is negatively regulated by Sam68 as it antagonizes the positive effects of SRSF1. We also show that the short isoform of *Rps6kb1*, namely, p31S6K1, is a potent repressor of adipogenesis, and its presence in Sam68-deficient prea-

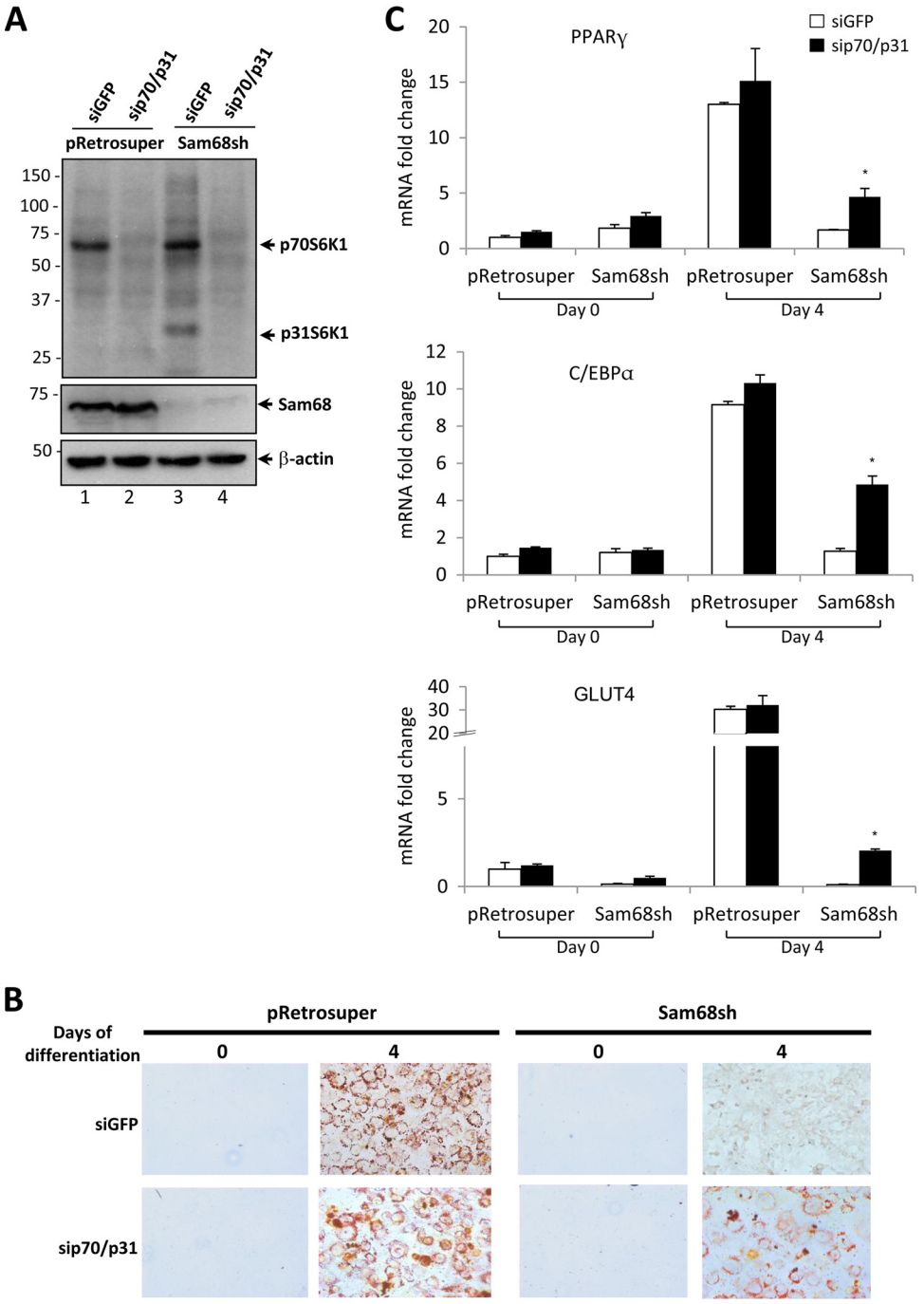

FIG 10 p31S6K1 contributes to the adipogenesis defects independently of the p70S6K1 isoform. (A) pRetrosuper or Sam68sh 3T3-L1 cells were transfected with siGFP (control) and sip70/p31. The protein extracts were immunoblotted with the indicated antibodies. β-Actin is shown as the loading control. Molecular mass markers are shown on the left in kilodaltons. (B) The cells indicated in panel A were induced to differentiate for 4 days. Adipocyte differentiation was assessed by Oil Red O staining. (C) The mRNA levels of PPARγ, C/EBPα, and GLUT4 normalized to 18S rRNA were assessed by RT-qPCR. The data are expressed as relative values from differentiation days 0 and 4. Error bars represent standard deviations of the means (*, $P < 0.05$).

dipocytes contributes to the adipogenesis defects observed in these cells.

ACKNOWLEDGMENTS

We thank Zhenbao Yu and Gillian Vogel for helpful discussions and for critically reading the manuscript.

The work was supported by a grant from the Canadian Institute of Health Canada (MOP-123531) to S.R.

REFERENCES

1. **Bielli P, Busà R, Paronetto MP, Sette C.** 2011. The RNA-binding protein Sam68 is a multifunctional player in human cancer. Endocr Relat Cancer **18:**R91-102. http://dx.doi.org/10.1530/ERC-11-0041.

2. **Richard S.** 2010. Reaching for the stars: linking RNA binding proteins to diseases. Adv Exp Med Biol **693:**142–157. http://dx.doi.org/10.1007/978-1-4419-7005-3_10.
3. **Galarneau A, Richard S.** 2009. The STAR RNA binding proteins GLD-1, QKI, SAM68 and SLM-2 bind bipartite RNA motifs. BMC Mol Biol **10:**47. http://dx.doi.org/10.1186/1471-2199-10-47.
4. **Lin Q, Taylor SJ, Shalloway D.** 1997. Specificity and determinants of Sam68 RNA binding. Implications for the biological function of K homology domains. J Biol Chem **272:**27274–27280.
5. **Matter N, Herrlich P, Konig H.** 2002. Signal-dependent regulation of splicing via phosphorylation of Sam68. Nature **420:**691–695. http://dx.doi.org/10.1038/nature01153.
6. **Cappellari M, Bielli P, Paronetto MP, Ciccosanti F, Fimia GM, Saarikettu J, Silvennoinen O, Sette C.** 2014. The transcriptional co-activator SND1 is a novel regulator of alternative splicing in prostate cancer cells. Oncogene **33:**3794–3802. http://dx.doi.org/10.1038/onc.2013.360.
7. **Bielli P, Busà R, Di Stasi SM, Munoz MJ, Botti F, Kornblihtt AR, Sette C.** 2014. The transcription factor FBI-1 inhibits SAM68-mediated BCL-X alternative splicing and apoptosis. EMBO Rep **15:**419–427. http://dx.doi.org/10.1002/embr.201338241.
8. **Paronetto MP, Achsel T, Massiello A, Chalfant CE, Sette C.** 2007. The RNA-binding protein Sam68 modulates the alternative splicing of Bcl-x. J Cell Biol **176:**929–939. http://dx.doi.org/10.1083/jcb.200701005.
9. **Valacca C, Bonomi S, Buratti E, Pedrotti S, Baralle FE, Sette C, Ghigna C, Biamonti G.** 2010. Sam68 regulates EMT through alternative splicing-activated nonsense-mediated mRNA decay of the SF2/ASF proto-oncogene. J Cell Biol **191:**87–99. http://dx.doi.org/10.1083/jcb.201001073.
10. **Chawla G, Lin CH, Han A, Shiue L, Ares MJ, Black DL.** 2009. Sam68 regulates a set of alternatively spliced exons during neurogenesis. Mol Cell Biol **29:**201–213. http://dx.doi.org/10.1128/MCB.01349-08.
11. **Iijima T, Wu K, Witte H, Hanno-Iijima Y, Glatter T, Richard S, Scheiffele P.** 2011. SAM68 regulates neuronal activity-dependent alternative splicing of neurexin-1. Cell **147:**1601–1614. http://dx.doi.org/10.1016/j.cell.2011.11.028.
12. **Pedrotti S, Bielli P, Paronetto MP, Ciccosanti F, Fimia GM, Stamm S, Manley JL, Sette C.** 2010. The splicing regulator Sam68 binds to a novel exonic splicing silencer and functions in SMN2 alternative splicing in spinal muscular atrophy. EMBO J **29:**1235–1247. http://dx.doi.org/10.1038/emboj.2010.19.
13. **Sellier C, Rau F, Liu Y, Tassone F, Hukema RK, Gattoni R, Schneider A, Richard S, Willemsen R, Elliott DJ, Hagerman PJ, Charlet-Berguerand N.** 2010. Sam68 sequestration and partial loss of function are associated with splicing alterations in FXTAS patients. EMBO J **29:**1248–1261. http://dx.doi.org/10.1038/emboj.2010.21.
14. **Paronetto MP, Messina V, Barchi M, Geremia R, Richard S, Sette C.** 2011. Sam68 marks the transcriptionally active stages of spermatogenesis and modulates alternative splicing in male germ cells. Nucleic Acids Res **39:**4961–4974. http://dx.doi.org/10.1093/nar/gkr085.
15. **Paronetto MP, Messina V, Bianchi E, Barchi M, Vogel G, Moretti C, Palombi F, Stefanini M, Geremia R, Richard S, Sette C.** 2009. Sam68 regulates translation of target mRNAs in male germ cells, necessary for mouse spermatogenesis. J Cell Biol **185:**235–249. http://dx.doi.org/10.1083/jcb.200811138.
16. **Huot ME, Vogel G, Zabarauskas A, Ngo CT, Coulombe-Huntington J, Majewski J, Richard S.** 2012. The Sam68 STAR RNA-binding protein regulates mTOR alternative splicing during adipogenesis. Mol Cell **46:**187–199. http://dx.doi.org/10.1016/j.molcel.2012.02.007.
17. **Laplante M, Sabatini DM.** 2012. mTOR signaling in growth control and disease. Cell **149:**274–293. http://dx.doi.org/10.1016/j.cell.2012.03.017.
18. **Dann SG, Selvaraj A, Thomas G.** 2007. mTOR Complex1-S6K1 signaling: at the crossroads of obesity, diabetes and cancer. Trends Mol Med **13:**252–259. http://dx.doi.org/10.1016/j.molmed.2007.04.002.
19. **Shimobayashi M, Hall M.** 2014. Making new contacts: the mTOR network in metabolism and signalling crosstalk. Nat Rev Mol Cell Biol **15:**155–162. http://dx.doi.org/10.1038/nrm3757.
20. **Inoki K, Zhu T, Guan KL.** 2003. TSC2 mediates cellular energy response to control cell growth and survival. Cell **115:**577–590. http://dx.doi.org/10.1016/S0092-8674(03)00929-2.
21. **Saucedo LJ, Gao X, Chiarelli DA, Li L, Pan D, Edgar BA.** 2003. Rheb promotes cell growth as a component of the insulin/TOR signalling network. Nat Cell Biol **5:**566–571. http://dx.doi.org/10.1038/ncb996.
22. **Tee AR, Manning BD, Roux PP, Cantley LC, Blenis J.** 2003. Tuberous sclerosis complex gene products, Tuberin and Hamartin, control mTOR signaling by acting as a GTPase-activating protein complex toward Rheb. Curr Biol **13:**1259–1268. http://dx.doi.org/10.1016/S0960-9822(03)00506-2.
23. **Wang L, Harris TE, Roth RA, Lawrence JCJ.** 2007. PRAS40 regulates mTORC1 kinase activity by functioning as a direct inhibitor of substrate binding. J Biol Chem **282:**20036–20044. http://dx.doi.org/10.1074/jbc.M702376200.
24. **Vander Haar E, Lee SI, Bandhakavi S, Griffin TJ, Kim DH.** 2007. Insulin signalling to mTOR mediated by the Akt/PKB substrate PRAS40. Nat Cell Biol **9:**316–323. http://dx.doi.org/10.1038/ncb1547.
25. **Thedieck K, Polak P, Kim ML, Molle KD, Cohen A, Jenö P, Arrieumerlou C, Hall M.** 2007. PRAS40 and PRR5-like protein are new mTOR interactors that regulate apoptosis. PLoS One **2:**e1217. http://dx.doi.org/10.1371/journal.pone.0001217.
26. **Sonenberg N, Hinnebusch AG.** 2009. Regulation of translation initiation in eukaryotes: mechanisms and biological targets. Cell **136:**731–745. http://dx.doi.org/10.1016/j.cell.2009.01.042.
27. **Carnevalli LS, Masuda K, Frigerio F, Le Bacquer O, Um SH, Gandin V, Topisirovic I, Sonenberg N, Thomas G, Kozma SC.** 2010. S6K1 plays a critical role in early adipocyte differentiation. Dev Cell **18:**763–774. http://dx.doi.org/10.1016/j.devcel.2010.02.018.
28. **Chen T, Boisvert FM, Bazett-Jones DP, Richard S.** 1999. A role for the GSG domain in localizing Sam68 to novel nuclear structures in cancer cell lines. Mol Biol Cell **10:**3015–3033. http://dx.doi.org/10.1091/mbc.10.9.3015.
29. **Sun Y, Ma YC, Huang J, Chen KY, McGarrigle DK, Huang XY.** 2005. Requirement of SRC-family tyrosine kinases in fat accumulation. Biochemistry **44:**14455–14462. http://dx.doi.org/10.1021/bi0509090.
30. **Huppertz I, Attig J, D'Ambrogio A, Easton LE, Sibley CR, Sugimoto Y, Tajnik M, König J, Ule J.** 2014. iCLIP: protein-RNA interactions at nucleotide resolution. Methods **65:**274–287. http://dx.doi.org/10.1016/j.ymeth.2013.10.011.
31. **Karni R, de Stanchina E, Lowe SW, Sinha R, Mu D, Krainer AR.** 2007. The gene encoding the splicing factor SF2/ASF is a proto-oncogene. Nat Struct Mol Biol **14:**185–193. http://dx.doi.org/10.1038/nsmb1209.
32. **Huot ME, Vogel G, Richard S.** 2009. Identification of a Sam68 ribonucleoprotein complex regulated by epidermal growth factor. J Biol Chem **284:**31903–31913. http://dx.doi.org/10.1074/jbc.M109.018465.
33. **Fu XD, Ares MJ.** 2014. Context-dependent control of alternative splicing by RNA-binding proteins. Nat Rev Genet **15:**689–701. http://dx.doi.org/10.1038/nrg3778.
34. **Witten JT, Ule J.** 2011. Understanding splicing regulation through RNA splicing maps. Trends Genet **27:**89–97. http://dx.doi.org/10.1016/j.tig.2010.12.001.
35. **Das S, Krainer AR.** 2014. Emerging functions of SRSF1, splicing factor and oncoprotein, in RNA metabolism and cancer. Mol Cancer Res **12:**1195–1204. http://dx.doi.org/10.1158/1541-7786.MCR-14-0131.
36. **Batsche E, Yaniv M, Muchardt C.** 2006. The human SWI/SNF subunit Brm is a regulator of alternative splicing. Nat Struct Mol Biol **13:**22–29. http://dx.doi.org/10.1038/nsmb1030.
37. **Ben-Hur V, Denichenko P, Siegfried Z, Maimon A, Krainer A, Davidson B, Karni R.** 2013. S6K1 alternative splicing modulates its oncogenic activity and regulates mTORC1. Cell Rep **3:**103–115. http://dx.doi.org/10.1016/j.celrep.2012.11.020.
38. **Schalm SS, Blenis J.** 2002. Identification of a conserved motif required for mTOR signaling. Curr Biol **12:**632–639. http://dx.doi.org/10.1016/S0960-9822(02)00762-5.
39. **Rosner M, Hengstschläger M.** 2011. Nucleocytoplasmic localization of p70 S6K1, but not of its isoforms p85 and p31, is regulated by TSC2/mTOR. Oncogene **30:**4509–4522. http://dx.doi.org/10.1038/onc.2011.165.
40. **Um SH, Frigerio F, Watanabe M, Picard F, Joaquin M, Sticker M, Fumagalli S, Allegrini PR, Kozma SC, Auwerx J, Thomas G.** 2004. Absence of S6K1 protects against age- and diet-induced obesity while enhancing insulin sensitivity. Nature **431:**200–205. http://dx.doi.org/10.1038/nature02866.